Magnetic order, spin correlations, and superconductivity in single-crystal $Nd_{1.85}Ce_{0.15}CuO_{4+\delta}$

M. Matsuda, Y. Endoh, and K. Yamada
Department of Physics, Tohoku University, Aramaki Aoba, Sendai 980, Japan

H. Kojima and I. Tanaka
Inorganic Synthesis Facility, Engineering Faculty, Yamanashi University, Kofu 200, Japan

R. J. Birgeneau and M. A. Kastner
Department of Physics, Massachusetts Institute of Technology, Cambridge, Massachusetts 02139

G. Shirane
Physics Department, Brookhaven National Laboratory, Upton, New York 11973
(Received 18 December 1991)

Measurements are reported of the static, instantaneous, and dynamic spin correlations in single crystals of $Nd_{1.85}Ce_{0.15}CuO_{4+\delta}$. The as-grown crystals show antiferromagnetic long-range order. However, the Néel temperatures and spin-stiffness constants are greatly reduced from their respective values in $Nd_2CuO_{4+\delta}$. After reduction and annealing, the crystals superconduct with $T_c = 23$ K, but inclusions of the antiferromagnetic phase, albeit with reduced Néel temperatures, are always present. Based on these data, we suggest that the disorder due to excess oxygen in as-grown samples stabilizes the magnetic correlations. This leads to a speculative model for the effects of deoxygenation in which the removal of the excess oxygen causes the magnetic correlations to diminish and hence superconductivity to become possible.

I. INTRODUCTION

Because holes carry the current in the majority of the high-temperature superconductors, the discovery[1] of the electron-doped cuprate superconductors, such as $Nd_{1.85}Ce_{0.15}CuO_{4+\delta}$, was taken as evidence that the CuO_2 layers, responsible for the superconductivity, displayed electron-hole symmetry. It has since become clear that the addition of electrons to the CuO_2 layers by doping $Nd_2CuO_{4+\delta}$ with Ce has very different consequences from that of introducing holes by doping $La_2CuO_{4+\delta}$ with Sr. In particular, the magnetic long-range order is destroyed in $La_{2-x}Sr_xCuO_{4+\delta}$ for $x \geq 0.02$ to be replaced by highly inelastic two-dimensional (2D) spin fluctuations; for $0.02 \lesssim x \lesssim 0.05$, spin-glass behavior is observed.[2] In contrast, three-dimensional (3D) magnetic long-range order in $Nd_{2-x}Ce_xCuO_{4+\delta}$ and $Pr_{2-x}Ce_xCuO_{4+\delta}$ persists[1,3] to $x \sim 0.15$.

In this paper we report experiments designed to explore in greater detail the destruction of long-range order and the emergence of superconductivity in single crystals of $Nd_{1.85}Ce_{0.15}CuO_{4+\delta}$. We present neutron-scattering measurements of the static, instantaneous, and dynamic spin correlations of such single crystals before and after annealing in Ar to reduce δ. Before this reducing step, the crystals have 3D long-range antiferromagnetic order, and their 2D spin correlations in the paramagnetic phase have the renormalized classical behavior predicted by theory with a spin stiffness which depends on x and, presumably, δ. Removal of oxygen drives the system into the superconducting phase. However, no annealing procedure was found which would entirely eliminate the antiferromagnetic phase.

II. EXPERIMENTAL RESULTS

Single crystals of $Nd_{1.85}Ce_{0.15}CuO_{4+\delta}$ were grown by a floating-zone technique described elsewhere.[4] Typical crystals have a volume of about 0.5 cm^3. The concentrations of Nd, Ce, and Cu were determined by electron microprobe analysis; however, the deviation δ from oxygen stoichiometry is unknown, although various chemical analyses[5] suggest that δ may be as large as 0.04.

Neutron-scattering experiments were performed at the two Tohoku University three-axis spectrometers (TOPAN and TUNS) at the Japan Atomic Energy Research Institute. The resolution functions of these two spectrometers were slightly different. In each spectrometer a pyrolytic graphite single crystal was used as a monochromator, and contamination from higher-order reflections was reduced using a pyrolytic graphite filter. For the two-axis experiments described here, the incident neutron energy was 30 meV; for the triple-axis measurements, the final neutron energy was fixed at 14.7 meV.

The magnetic Bragg scattering as well as the inelastic spin fluctuations were measured using the three-axis configuration, in which one measures both the initial and final neutron energy as well as the momentum transfer; for the Bragg scattering, the energy transfer was fixed at zero. To measure the 2D antiferromagnetic correlation

length in the paramagnetic phase, one must measure the instantaneous correlation function. This is accomplished in a configuration in which the outgoing neutrons have their wave vectors perpendicular to the CuO_2 layers and in which the analyzer is removed, so that neutrons of all energies are collected.[2] In this paper all data are indexed on the magnetic rather than the chemical unit cell. Thus the 2D antiferromagnetic rods of scattering occur along $(10l)$, $(30l)$, etc.

Magnetic shielding measurements were made on single crystals in the superconducting state. A vibrating-sample magnetometer was used to measure the magnetic moment of the crystals as a function of temperature in a field of 10 Oe after cooling in zero field. We now discuss the neutron results.

A. As-grown crystals

The crystal and magnetic structures of pure $Nd_2CuO_{4+\delta}$ are shown in Fig. 1.[6] Nearest-neighbor Cu^{2+} spins in the CuO_2 sheets are ordered antiferromagnetically. The 3D order is such that the spin direction **S** is along the 3D antiferromagnetic propagation direction τ. There is, in addition, a moment induced by the Cu-Nd interaction on the Nd^{3+} site as shown in the figure. $Nd_2CuO_{4+\delta}$ has the magnetic structure shown in Fig. 1 for temperatures $255 > T > 75$ K and $30\text{ K} > T$. In the intermediate-temperature range, the spin reorients so that $\mathbf{S} \perp \tau$. Matsuda *et al.*[6] speculate that the spin-reorientation transitions arise from a competition between the Cu^{2+}-Cu^{2+} and Cu^{2+}-Nd^{3+} interlayer interactions, with the latter changing with temperature because of the depopulation of the Nd^{3+} crystal-field levels.

We find, generally, that as-grown crystals of $Nd_{1.85}Ce_{0.15}CuO_{4+\delta}$ have Néel temperatures in the range 125–160 K, presumably because of varying δ's. Figure 2 shows the intensity of the (101) and (103) magnetic Bragg peaks as functions of temperature for a sample with $T_N \sim 125$ K. From Fig. 2 it is evident that this sample exhibits only the magnetic phase shown in Fig. 1 with no intermediate spin-reorientation transitions. For the structure shown in Fig. 1, the intensities of the (101) and (103) peaks are given by[6]

$$I(101) \sim (M_{Cu} f_{Cu} - 1.2 M_{Nd} f_{Nd})^2 ,$$
$$I(103) \sim (M_{Cu} f_{Cu} + 1.9 M_{Nd} f_{Nd})^2 , \quad (1)$$

where M and f represent the ordered staggered moment and form factor of the Cu^{2+} and Nd^{3+} ions. Using Eq. (1), one may deduce the Cu^{2+} and Nd^{3+} moments separately. These are shown in the lower panel in Fig. 2. Presumably the Nd moments become fully ordered at a temperature lower than 10 K. Identical behavior is observed in other samples of $Nd_{1.85}Ce_{0.15}CuO_{4+\delta}$ with varying Néel temperatures.

It is now well established that the paramagnetic spin correlations within the CuO_2 layers for the pure materials are well described by the 2D $S = \frac{1}{2}$ Heisenberg model.[7] Three-dimensional long-range order results from the small XY anisotropy and weak interlayer coupling.[6] In the paramagnetic phase of such crystals, the large nearest-neighbor exchange results in antiferromagnetic correlations with a relatively long length scale ξ.

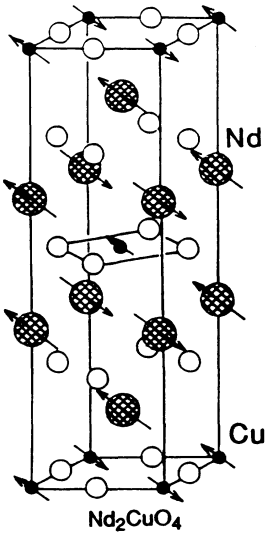

FIG. 1. Crystal and magnetic structure of $Nd_2CuO_{4+\delta}$ for $75 < T < 255$ K and $T < 30$ K. In the intermediate-temperature range $30 < T < 75$ K, the spin direction is rotated by 90° in the CuO_2 plane.

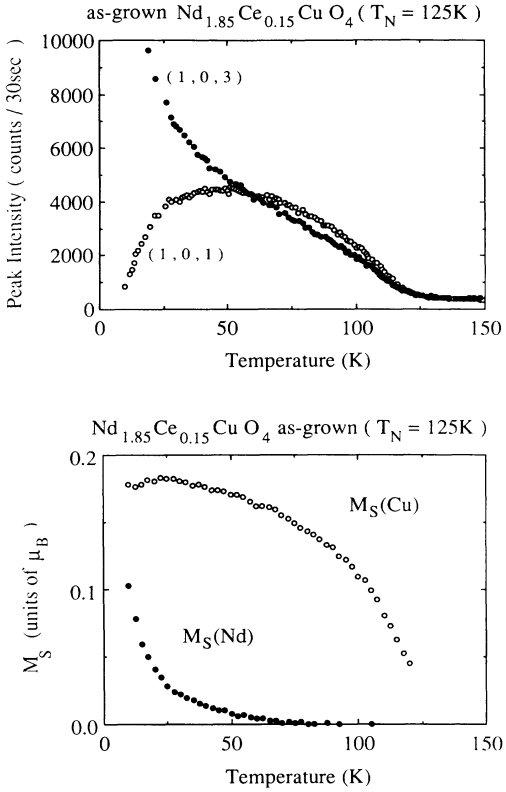

FIG. 2. Upper panel: temperature dependence of (101) and (103) Bragg peaks. Lower panel: staggered moments for Cu and Nd spins extracted from the Bragg peaks using the analysis of Ref. 6.

As described above, the instantaneous correlations are measured using a two-axis configuration. Scans along h through $(10l)$ yield single (commensurate) Lorentzians whose half width at half maximum is just ξ^{-1}. Representative data for a sample with $T_N = 160$ K are shown in Fig. 3. As may be seen from the figure, these experiments are much more difficult than those in La_2CuO_4 (Refs. 2 and 7) because of the large background from the Nd^{3+} paramagnetic scattering. The inverse correlation lengths ξ^{-1} determined from such two-axis scans are shown in Fig. 4 for two as-grown crystals of $Nd_{1.85}Ce_{0.15}CuO_{4+\delta}$; also shown are data for $Nd_2CuO_{4+\delta}$ from Thurston *et al.*[8] For the 2D $S=\frac{1}{2}$ Heisenberg model, theory predicts renormalized classical behavior:[9]

$$\xi = \frac{e}{8}\frac{\hbar c}{2\pi\rho_s}\left[1-0.5\frac{kT}{2\pi\rho_s}\right]\exp(2\pi\rho_s/kT)\ , \qquad (2)$$

where $\hbar c$ is the spin-wave velocity and ρ_s is the spin stiffness. In the pure system, the renormalized spin-stiffness constant ρ_s is simply related to the nearest-neighbor exchange J by $2\pi\rho_s = \alpha J$, where spin-wave theory predicts[9] $\alpha = 0.94$, and the best fit to the data used for La_2CuO_4 gives[10] $\alpha = 1.1$. For La_2CuO_4 containing no holes, Keimer *et al.*[10] find $2\pi\rho_s \sim 150$ meV. For undoped $Nd_2CuO_{4+\delta}$ ($T_N = 255$ K), the value from Thurston *et al.*[8] ($2\pi\rho_s \sim 130$ meV) in Eq. (2) gives the solid line for the undoped crystal in Fig. 4. Our data for ξ^{-1} in the doped samples are clearly very limited. Nevertheless, as is evident from Fig. 4, they are at least consistent with Eq. (2), but with reduced values for the spin-stiffness constants ρ_s. Specifically, for the two Ce-doped crystals, we find $2\pi\rho_s \sim 70$ meV ($T_N = 160$ K) and ~ 50 meV ($T_N = 125$ K), respectively. Thurston *et al.*[8] found $2\pi\rho_s \sim 80$ meV for $Pr_{1.92}Ce_{0.08}CuO_{4+\delta}$ ($T_N = 170$ K), demonstrating that the suppression of $2\pi\rho_s$ with Ce doping is a general phenomenon and that both $2\pi\rho_s$ and T_N decrease in unison. This behavior for ξ^{-1} is an important result whose significance we shall discuss in Sec. III.

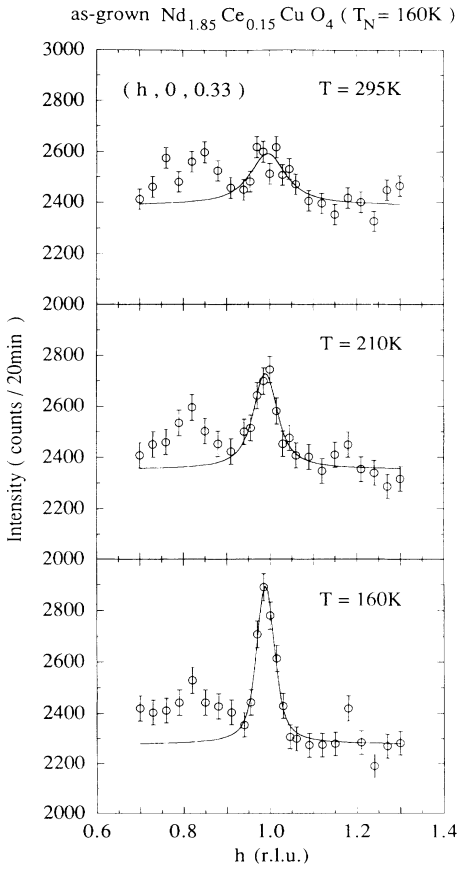

FIG. 3. Two-axis scans across the 2D rod (h,0,0.33) for as-grown $Nd_{1.85}Ce_{0.15}CuO_4$ with $T_N = 160$ K. The spectrometer configuration was open-30′-*S*-60′. The peak at $h = 0.8$ is due to an impurity phase. The solid lines are the results of fits to a 2D Lorentzian convoluted with the instrumental resolution function.

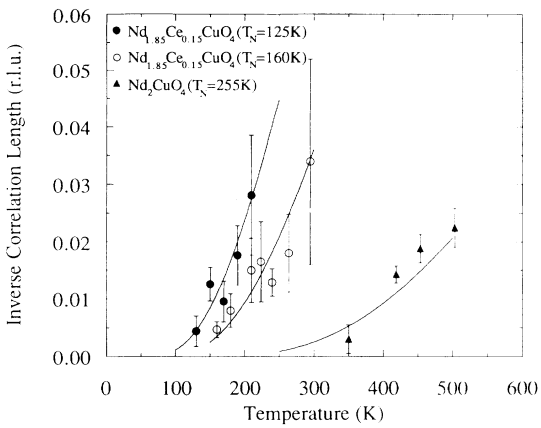

FIG. 4. Inverse correlation lengths vs temperature for two as-grown Ce-doped single crystals. Data for Nd_2CuO_4 are from Ref. 8. The solid lines correspond to Eq. (2), with $2\pi\rho_s = 50$ meV ($T_N = 125$ K), 70 meV ($T_N = 160$ K), and 150 meV (pure system), respectively.

Representative inelastic data at 6 meV in an as-grown sample with $T_N = 160$ K are shown in Fig. 5. In these measurements the energy transfer was fixed at 6 meV, the out-of-plane wave vector was held at $l = -1.1$ and the in-plane wave vector h was scanned through the (1,0, -1.1) position. The spectrometer configuration was 40′-60′-*S*-60′-80′, with the outgoing neutron energy E_f fixed at 14.7 meV. As may be seen in Fig. 5, resolution-limited peaks centered about $h = 1$ were indeed observed. However, the signal-to-noise ratio was poor because of the large q-independent background arising from the Nd^{3+} paramagnetic scattering.[11] The Nd^{3+} ions gave rise to a background which varied significantly with both energy and temperature and, unfortunately, was quite important in the energy range of interest here.[11] Nevertheless, one could reasonably estimate the relative magnitude and temperature dependence of the inelastic scattering. Data so obtained at 3, 6, and 9 meV for temperatures between 10 and 300 K are shown in Fig. 6. This temperature variation mimics rather well the behavior found by Yamada *et al.*[7] in pure La_2CuO_4 (see their Fig.

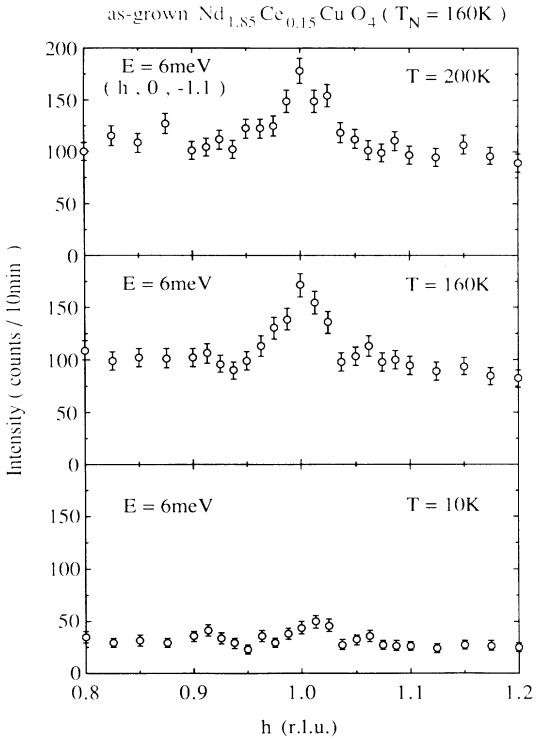

FIG. 5. Three-axis scans across the 2D rod at an energy transfer of 6 meV along $(h, 0, -1.1)$ for three temperatures in an as-grown crystal. The spectrometer configuration was 40′-60′-S-60′-80′, with E_f fixed at 14.7 meV.

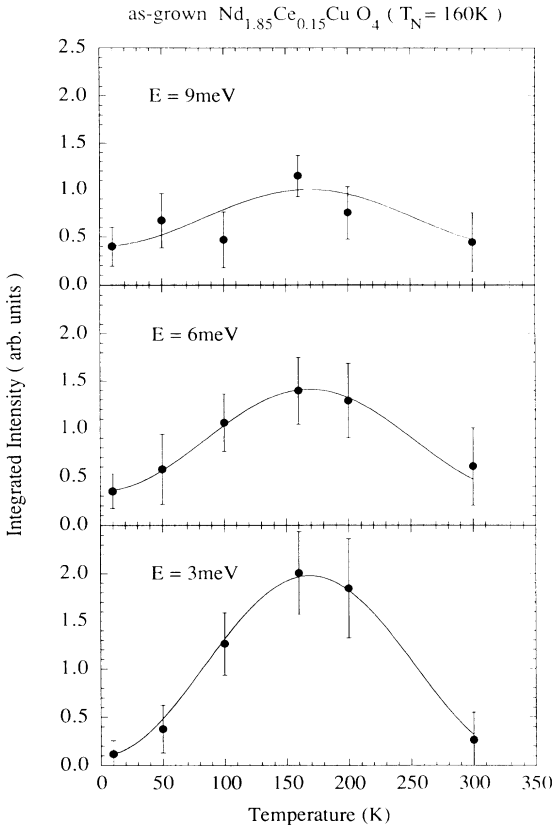

FIG. 6. Integrated inelastic intensity vs temperature at energies of 3, 6, and 9 meV in an as-grown crystal with $T_N = 160$ K. The solid lines are guides to the eye.

9). Thus the basic character of the spin dynamics does not seem to be appreciably changed by the doping.

In summary, as-grown samples of $Nd_{1.85}Ce_{0.15}CuO_{4+\delta}$ exhibit Néel ordering, instantaneous spin correlations, and spin dynamics which are isomorphous to those in the pure materials. The only notable difference is that the spin stiffness ρ_s and, hence, the temperature scale are significantly diminished by the Ce doping. As we shall now discuss, the effects of deoxygenation are much more drastic.

B. Reduced and annealed crystals

The crystals were subjected to various heat treatments in reducing and oxidizing ambients in an effort to convert them as thoroughly as possible to the superconducting phase. The most effective of these was a 20-h reduction in Ar at 950 °C followed by a 20-h anneal in oxygen at 500 °C, although it should be emphasized that the efficiency of the reduction process was sample dependent. Figure 7 (lower panel) shows the (101) magnetic Bragg peak for one of the crystals before and after this procedure. The as-grown crystal in this case had a Néel temperature of 160 K. After reduction and annealing, the magnetically ordered component was reduced to about 30% of its initial value; the Néel temperature of this residual phase was ~80 K. Results for a second crystal are shown in Fig. 8. In this case there is a residual antiferromagnetic phase of relative volume ~0.1. In none of the crystals and by none of the reduction and annealing procedures were we able to reduce the magnetically ordered fraction by more than a factor ~10.

After reduction and annealing, the crystals displayed the superconducting transition seen in the shielding measurements in the upper panels of Figs. 7 and 8. These are results for the same samples for which the Bragg-peak measurements are given in the lower panels. The magnetic moments in both samples show the onset of superconductivity at 23 K and transitions which are a few K wide. Because the samples contained material that is not part of the single crystal and because of the irregular shape of the sample, it was not possible to determine the Meissner fraction quantitatively, although it is unambiguous that we were observing bulk superconductivity.

Several crystals were reduced and annealed for various lengths of time. It appears that the fraction of coexisting antiferromagnetic phase remaining varies more from one crystal to the next than it does with heat treatment. However, the superconducting T_c is independent of the Néel temperature of the as-grown crystal. It thus appears that the superconducting phase is always the same, even though its volume fraction varies from sample to sample. It is important to note that such detailed information about sample homogeneity is not available in any of the many other studies of superconductivity in the $Nd_{2-x}Ce_xCuO_{4+\delta}$ system.[5,12] Thus much of the varia-

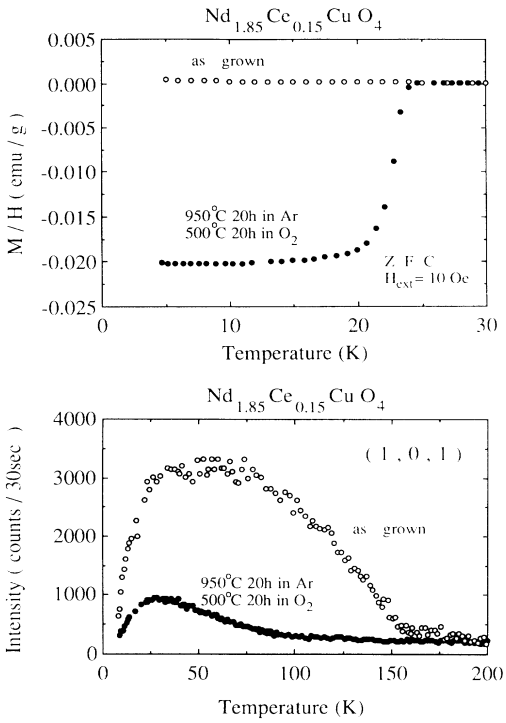

FIG. 7. Upper panel: M/H vs temperature after reduction and annealing. The sample was cooled in zero magnetic field. Lower panel: (101) Bragg-peak intensity before and after reduction and annealing. The same single crystal was used for all measurements as well as those in Figs. 3, 5, and 6.

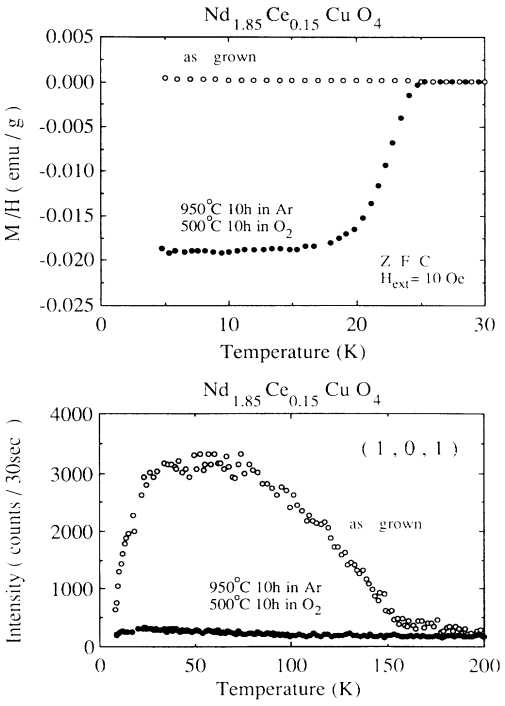

FIG. 8. Upper panel: M/H vs temperature both before and after reduction and annealing. The samples were cooled in zero magnetic field. Lower panel: (101) Bragg-peak intensity before and after reduction and annealing. The as-grown data are from Fig. 7. The superconducting sample data are for a second crystal, which was only studied after reduction and annealing.

bility in results between different groups and indeed some of the outright contradictions may originate from improperly assessed inhomogeneities.[12]

We carried out an extensive survey of the spin dynamics in the superconducting crystals. Representative results at 6 meV are shown in Fig. 9. These should be compared with the data in Fig. 5, which were carried out with the identical spectrometer configuration on a similar crystal before the annealing procedure. The background scan in Fig. 9 was measured by tilting the crystal around the scattering vector by 12°. As is evident in Fig. 9, we find *no magnetic signal* above the background to within the statistical error for the superconducting crystal (Fig. 8) containing $\sim 10\%$ of the antiferromagnetic phase.

Unfortunately, because of the high background and concomitant low signal-to-noise ratio in the antiferromagnetic phase dynamical signal, one can only draw a weak conclusion from the data shown in Fig. 9. Specifically, if in the superconducting phase the inverse correlation length was increased to $\xi^{-1} \sim 0.1$ reciprocal-lattice units (r.l.u.), then no magnetic signal could be seen above the background; for example, with $\xi^{-1} \sim 0.1$ r.l.u. and an integrated signal comparable to that in Fig. 5, one could have a maximum signal of ten counts at the peak for the scans shown in Fig. 9. Such a signal could clearly not be separated from the background in a reasonable

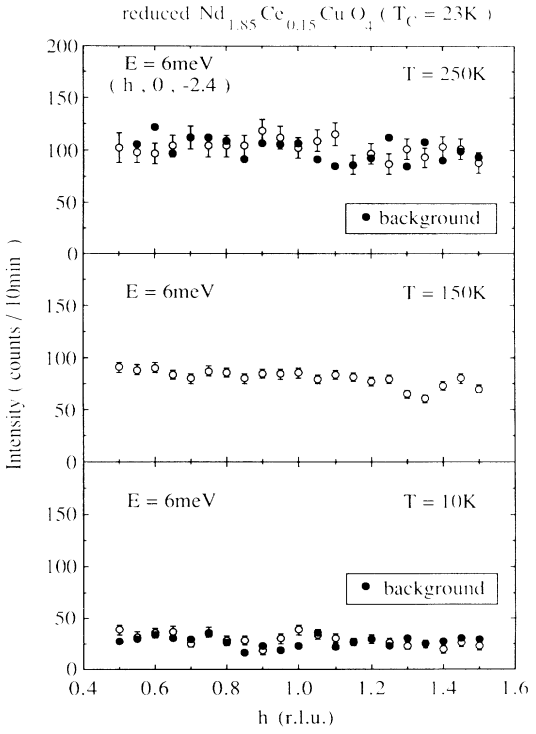

FIG. 9. Three-axis scans across the 2D rod at an energy transfer of 6 meV in a sample which had been reduced and annealed. The background scans were obtained by tilting the crystal by 12°. The sample was the same as that used to obtain the superconducting data shown in Fig. 8. The spectrometer configuration was 40′-60′-*S*-60′-80′, with E_f fixed at 14.7 meV.

counting time. Thus we can only say that in superconducting samples of $Nd_{1.85}Ce_{0.15}CuO_4$ the inverse magnetic correlation length and/or any incommensurability must be of order 0.1 r.l.u. or greater. This is comparable to values in the hole-doped superconductors.[13]

III. DISCUSSION AND CONCLUSIONS

To understand fully the implications of our results on the single-layer electron-doped material $Nd_{1.85}Ce_{0.15}CuO_{4+\delta}$, it is useful to compare them with those for the single-layer hole-doped material $La_{2-x}Sr_xCuO_{4+\delta}$. As demonstrated in the recent work of Keimer *et al.*,[14] the reduction of T_N by Ce doping in $Pr_{2-x}Ce_xCuO_4$ is much more gradual than that by oxygen or Sr doping in $La_{2-x}Sr_xCuO_{4+\delta}$. In the former T_N decreases at a rate of ~ 9 K/at. %, extrapolating to zero at $\sim 25\%$ Ce, whereas in the latter the rate is ~ 160 K/at. %, extrapolating to zero at $\sim 2\%$ hole concentration. Using the values of T_N measured here for $Nd_{1.85}Ce_{0.15}CuO_{4+\delta}$, we find a rate in good agreement with the results for $Pr_{2-x}Ce_xCuO_{4+\delta}$. Keimer *et al.*[14] also showed that Zn doping of La_2CuO_4 reduces T_N at the same rate as Ce doping of $Pr_{2-x}Ce_xCuO_{4+\delta}$. Since Zn substitutes for Cu but has one more valence electron, its addition increases the number of electrons in the CuO_2 layer, as presumably does Ce doping in $Pr_{2-x}Ce_xCuO_{4+\delta}$ and $Nd_{2-x}Ce_xCuO_{4+\delta}$.[15] However, in the case of Zn doping, the electron is tightly bound, whereas the nearly metallic conductivity resulting from Ce doping suggests that the electrons in the latter case are more mobile.[12]

Figure 4 illustrates a second remarkable difference between the magnetic properties of the electron- and hole-doped materials. Doping with Ce clearly reduces the spin-stiffness constant from the value it has in the undoped material. However, no such reduction happens in the case of La_2CuO_4 doped with Sr or O. In the latter the correlation length at high temperatures is essentially unchanged by doping. For example, the inverse correlation length at 500 K is 0.02 r.l.u. in a crystal with $T_N=325$ K, which contains no excess holes and is only $\sim 10\%$ larger at the same temperature in a crystal doped with oxygen, to give $T_N=100$ K.[16] Birgeneau *et al.*[10] recently reported that even in crystals in which there is no 3D long-range order, the high-temperature behavior of the correlation length is essentially unchanged, following

$$\xi^{-1}=\xi_0^{-1}+\xi_{\text{pure}}^{-1}, \tag{3}$$

where ξ_{pure}^{-1} is the temperature-dependent inverse correlation length of the undoped material [Eq. (2)] and ξ_0^{-1} is a temperature-independent inverse length determined by the hole density. Thus, even in crystals with 4% holes per Cu atom in which the 3D order is destroyed, one must raise the temperature to ~ 500 K to obtain inverse lengths ~ 0.02 r.l.u. larger than the zero-temperature value. By contrast, to reach an inverse correlation length of ~ 0.02 r.l.u. in $Nd_{1.85}Ce_{0.15}CuO_{4+\delta}$, one needs to raise the temperature to only ~ 200 K.

As discussed by Matsuda *et al.*,[6] the three-dimensional long-range-order transition temperature in Nd_2CuO_4 is determined primarily by the weak XY anisotropy term in the spin Hamiltonian. The Néel temperature can be estimated by $(\xi/a)^2 J_{XY}\sim kT_N$, where J_{XY} is the XY anisotropy and a is the nearest-neighbor Cu-Cu distance; because of the exponential dependence of ξ on ρ_s/T [Eq. (2)], T_N will approximately scale with $2\pi\rho_s$. Thus the observed suppression of $2\pi\rho_s$ by a factor of ~ 2 is consistent with the suppression of T_N from ~ 255 to ~ 125 K.

Keimer *et al.*[14] suggested that, notwithstanding the differences in transport properties between $La_2Cu_{1-y}Zn_yO_4$ and $Pr_{2-x}Ce_xCuO_{4+\delta}$, the addition of electrons leads, in both cases, to dilution of the Cu spin system. On the other hand, Aharony *et al.*[17] suggested that hole doping leads to frustration. Similar ideas were proposed by Luke *et al.*[3] The behavior illustrated in Fig. 4 of the correlation length in $Nd_{2-x}Ce_xCuO_{4+\delta}$ is consistent with the idea that electron doping results in dilution. It is of interest to carry this intuitive idea one step further to determine the quantitative implications.

The magnetic behavior of diluted lattices has been discussed extensively by Harris and Kirkpatrick.[18] In particular, they have determined the dependence of ρ_s on dilution for various lattices. The results for the square lattice are shown in Fig. 3 of their paper. For a simple square lattice with nearest-neighbor interactions $\rho_s(p)\simeq[1-3.1(1-p)]\rho_s(1)$, where p is the fraction of sites occupied by a spin and $\rho_s(p)$ approaches zero for $p=0.593$, the nearest-neighbor square-lattice-site percolation threshold. Thus, from the data for ρ_s shown in Fig. 4, we may extract an effective Cu^{2+} spin density p_{eff} in each sample. For pure $Nd_2CuO_{4+\delta}$, by definition, $p=1$. For the sample with $T_N=160$ K, we have $\rho_s(160\text{ K})/\rho_s(255\text{ K})=\frac{800}{1400}=0.57$. From the above equation for $\rho_s(p)/\rho_s(1)$, this corresponds to a dilution $1-p_{\text{eff}}\simeq 0.14$. This is in remarkably good agreement with the measured Ce concentration of 0.15. For the sample with $T_N=125$ K, one has $\rho_s(p)/\rho_s(1)=\frac{600}{1400}=0.43$, which corresponds to $(1-p_{\text{eff}})=0.21$ Thus the reduction of T_N from 160 to 125 K, presumably due to partial deoxygenation, involves a significant increase in the effective (but not real) carrier concentration.

Since we do not know the precise oxygen content for each of our samples, our interpretation of the above results must be speculative. All of the data suggest that in the $Nd_{2-x}Ce_xCuO_4$ system for $x\leq 0.15$ the magnetism in as-grown samples may be understood quantitatively on the basis of simple site dilution. This implies that, to a first approximation for each Ce ion, a Cu^{2+} $S=\frac{1}{2}$ ion is converted to a localized Cu^{1+} $S=0$ ion, in agreement with the arguments of Tranquada *et al.*[15] and others.[19] This behavior is completely different from what one would have expected based on naive one-electron band-structure calculations, be they one or three band. However, even in a quasilocalized correlated-electron picture, it is quite surprising that the added electrons are not more effective in destroying the planar CuO_2 magnetism. As may be seen by considering the Nd_2CuO_4 structure (Fig. 1), one would have expected the added electron from the Ce dopant to be shared equally between the four

Cu sites which are symmetrically placed in the plane nearest the Ce-dopant site. This should destroy the antiferromagnetic order in the four sites in the plaquette and, further, should generate frustration with respect to the more distant Cu^{2+} neighbors.[20] The fact that this does not occur suggests that the added electron is predominantly localized on a single Cu^{2+} site. This can only happen if the local square symmetry about the Ce dopant is broken by the disorder.

Chemical analysis measurements indicate that the change in oxygen density on deoxygenation is quite small.[5] Thus the concomitant change in electron density in the CuO_2 planes must also be small, probably of order 1% or 2% for the carrier concentration in the CuO_2 planes. The simplest possible model for the dramatic effects of deoxygenation is that for a carrier concentration of order 0.15 per Cu; there is a first-order transition from a weakly localized doped Mott antiferromagnet to a highly correlated metallic and, at low temperatures, superconducting state. Our data by themselves are consistent with this scenario. However, this model would leave two major problems unresolved. First, it does not provide an explanation for the fact that the antiferromagnetic state is stable for carrier concentrations as high as ~ 0.15. Second, the model does not explain why only deoxygenation and not increased Ce concentration produces the superconductivity. Thus a more novel mechanism seems to be required. Accordingly, we propose the following simple, albeit highly speculative, model for the role of deoxygenation in these materials.

There is, by now, quite persuasive evidence that as-grown samples have an excess of oxygen.[5,21] Quite plausibly, these excess oxygens will sit at the empty apical sites (Fig. 1). This would serve to break the symmetry for all nearest- and next-nearest-neighbor Cu plaquettes. This in turn could serve to localize the dopant electrons primarily on one Cu site—hence the good agreement of $2\pi\rho_s(x)$ with the predictions of the site-percolation model. In this picture the effects of deoxygenation are clear. Removing the apical oxygens by deoxygenation would tend to restore the square symmetry about the Ce-dopant sites. (We are implicitly assuming here that the disorder due to the surrounding Ce ions is less important.) This in turn would cause the dopant electrons to be equally shared by the four Cu ions in the plaquette. For a dopant concentration of 0.15, one would then be beyond the plaquette percolation threshold (~ 0.1) and the long-range Cu^{2+} magnetic correlations would be destroyed. Concomitantly, the normal-state conductivity would increase and superconductivity would become allowed. This phenomenological picture appears to be consistent with all data in the literature. In this approach an optimal reduction-anneal procedure would be one which removes all of the interstitial oxygens but leaves the CuO_2 lattice intact.

In summary, we have shown that as-grown samples of $Nd_{1.85}Ce_{0.15}CuO_4$ show magnetic ordering together with static and dynamic spin correlations which can be understood quantitatively with a simple site-dilution model. The empirical effect of deoxygenation is to inhibit the magnetic correlations so that the inverse magnetic correlation length is at least 0.1 r.l.u. Superconductivity then occurs in this highly disordered magnetic state. We have proposed a speculative model for the microscopic effects of the deoxygenation process. Specifically, we suggest that the disordering potential of the interstitial oxygens in as-grown samples tends to localize the doped electrons onto single Cu sites, thence stabilizing the magnetic correlations. The principal role of deoxygenation then would be to remove this disordering potential from the apical oxygens, thus restoring the symmetry about the Cu plaquette and, in turn, destroying the Cu^{2+} magnetic correlations. In this highly disordered magnetic state, superconductivity would presumably be allowed. Clearly, further neutron measurements, especially on superconducting samples, are required to develop our empirical description further. Careful measurements of transport properties, including the Hall conductance in particular, on the single crystals before and after deoxygenation are also required.

ACKNOWLEDGMENTS

We would like to acknowledge stimulating conversations with Amnon Aharony, John Graybeal, Rick Greene, Brooks Harris, Bernhard Keimer, and N. P. Ong. The work at Tohoku University has been supported under a Grant-in-Aid in Scientific Research by the Ministry of Education, Science and Culture. The research at MIT was supported by the National Science Foundation under Grant Nos. DMR 90-22933 and DMR 90-07825. The work at Brookhaven National Laboratory was carried out under Contract No. DE-AC02-76CH00016 Division of Materials Science, U.S. Department of Energy. This study was supported in part by the U.S.-Japan Collaborative Program on Neutron Scattering.

[1]Y. Tokura, H. Takagi, and S. Uchida, Nature (London) **377**, 345 (1989); H. Takagi, S. Uchida, and Y. Tokura, Phys. Rev. Lett. **62**, 1197 (1989).

[2]For a review of magnetic properties, see R. J. Birgeneau and G. Shirane, in *Physical Properties of High Temperature Superconductors,* edited by D. M. Ginsberg (World Scientific, Singapore, 1989).

[3]G. M. Luke, B. J. Sternlieb, Y. J. Uemura, J. H. Brewer, R. Kadono, R. F. Kiefl, S. R. Kreitzman, T. M. Riseman, J. Gopalakrishnan, A. W. Sleight, M. A. Subramanian, S. Uchida, H. Takagi, and Y. Tokura, Nature (London) **338**, 49 (1989); G. M. Luke, L. P. Le, B. J. Sternlieb, Y. J. Uemura, J. H. Brewer, R. Kadono, R. F. Kiefl, S. R. Kreitzman, T. M. Riseman, C. E. Stronach, M. R. Davis, S. Uchida, H. Takagi, Y. Tokura, Y. Hidaka, T. Murakami, J. Gopalakrishnan, A. W. Sleight, M. A. Subramanian, E. A. Early, J. T. Markert,

M. B. Maple, and C. L. Seaman, Phys. Rev. B **42**, 7981 (1990).

[4]I. Tanaka and H. Kojima, Nature (London) **337**, 21 (1989).

[5]E. Moran, A. I. Nazzal, T. C. Huang, and J. B. Torrance, Physica C **160**, 30 (1989); E. Wang, J.-M. Tarascon, L. H. Greene, G. W. Hull, and W. R. McKinnon, Phys. Rev. B **41**, 6582 (1990); for similar results, albeit with a different interpretation, see K. Suzuki, K. Kishio, T. Hasegawa, and K. Kitazawa, Physica C **166**, 357 (1990).

[6]M. Matsuda, K. Yamada, K. Kakurai, H. Kadowaki, T. R. Thurston, Y. Endoh, Y. Hidaka, R. J. Birgeneau, M. A. Kastner, P. M. Gehring, A. H. Moudden, and G. Shirane, Phys. Rev. B **42**, 10 098 (1990).

[7]K. Yamada, K. Kakurai, Y. Endoh, T. R. Thurston, M. A. Kastner, R. J. Birgeneau, G. Shirane, Y. Hidaka, and T. Murakami, Phys. Rev. B **40**, 4557 (1989).

[8]T. R. Thurston, M. Matsuda, K. Kakurai, K. Yamada, Y. Endoh, R. J. Birgeneau, P. M. Gehring, Y. Hidaka, M. A. Kastner, T. Murakami, and G. Shirane, Phys. Rev. Lett. **65**, 263 (1990).

[9]S. Chakravarty, B. I. Halperin, and D. R. Nelson, Phys. Rev. B **39**, 2344 (1989); P. Hasenfratz and F. Niedermeyer, Phys. Lett. B **268**, 231 (1991).

[10]B. Keimer *et al.* (unpublished work); R. J. Birgeneau, N. Belk, Y. Endoh, R. W. Erwin, M. A. Kastner, B. Keimer, and G. Shirane, Physica B (to be published).

[11]A. T. Boothroyd, S. M. Doyle, D. McK. Paul, D. S. Misra, and R. Osborn, Physica C **165**, 17 (1990); A. Furrer, P. Allenspach, J. Mesot, and U. Staub, *ibid.* **168**, 609 (1990).

[12]Z. Z. Wang, T. R. Chien, N. P. Ong, J. M. Tarascon, and E. Wang, Phys. Rev. B **43**, 3020 (1991); S. J. Hagen, J. L. Peng, Z. Y. Li, and R. L. Greene, *ibid.* **43**, 13 606 (1991); S. Kohiki, J. Kawai, T. Kamada, S. Hayashi, H. Adachi, K. Setsune, and K. Wasa, Physica C **166**, 437 (1990).

[13]R. J. Birgeneau, Y. Endoh, K. Kakurai, Y. Hidaka, T. Murakami, M. A. Kastner, T. R. Thurston, G. Shirane, and K. Yamada, Phys. Rev. B **39**, 2868 (19894

[14]Y. Endoh, R. W. Erwin, M. A. Kastner, and G. Shirane, Phys. Rev. B **45**, 7430 (1992).

[15]J. M. Tranquada, S. M. Heald, A. R. Moodenbaugh, G. Liang, and M. Croft, Nature (London) **337**, 720 (1989).

[16]B. Keimer, Ph.D. thesis, Massachusetts Institute of Technology, 1991.

[17]A. Aharony, R. J. Birgeneau, A. Coniglio, M. A. Kastner, and H. E. Stanley, Phys. Rev. Lett. **60**, 1330 (1988).

[18]A. B. Harris and S. Kirkpatrick, Phys. Rev. B **16**, 542 (1977).

[19]See for example H. Oyanagi, Y. Yokoyama, H. Yamaguchi, Y. Kuwahara, T. Katayama, and Y. Nishihara, Phys. Rev. B **42**, 10 136 (1990).

[20]A. Aharony (private communication).

[21]As additional evidence, we have recently found that as-grown samples of $La_{1.6}Nd_{0.4}CuO_{4+\delta}$ have a hole concentration in excess of 2%, implying an excess-oxygen concentration per Cu of at least this value. As-grown La_2CuO_4 typically has $\sim 0.5\%$ excess holes.